CO$_2$QUEST Newsletter

Summer 2015

CO$_2$QUEST
Impact of the Quality of CO$_2$ on Storage and Transport

Introduction

Welcome to the third edition of the EU FP7-funded-project CO$_2$QUEST newsletter, highlighting the most recent technical developments since the project's commencement in March 2013. The CO$_2$QUEST consortium, led by Prof. Haroun Mahgerefteh at University College London (UCL, UK) comprises 10 other partners: Bundesanstalt für Geowissenschaften und Rohstoffe (BGR, Germany), Uppsala University (UU, Sweden), Dalian University of Technology (DUT, PR China), Environmental & Water Resources Engineering Ltd. (EWRE, Israel), Imperial College London (ICL, London), Institut National de l'Environnement Industriel et des Risques (INERIS, France), National Centre for Scientific Research 'Demokritos' (NCSRD, Greece), Onderzoekscentrum voor Aanwending van Staal (OCAS, Belgium), CanmetENERGY (CANMET, Canada) and the University of Leeds (UoL, UK).

CO$_2$QUEST addresses the fundamentally important issues regarding the impact of the typical impurities in the gas or dense-phase CO$_2$ stream captured from fossil fuel power plants on its safe and economic transportation and storage. The above involves the determination of the important CO$_2$ mixtures that have the most profound impact on the pipeline pressure drop, compressor power requirements, pipeline propensity to ductile and brittle facture propagation, corrosion of the pipeline and wellbore materials, geochemical interactions within the wellbore and storage site, and the ensuing health and environmental hazards. Based upon a cost/benefit analysis and whole system approach, the results will in turn be used to provide recommendations for tolerance levels, mixing protocols and control measures for pipeline networks and storage infrastructure.

University College London, UK

Bundesanstalt fur Geowissenschaften und Rohstoffe, Germany

Uppsala Universitet, Sweden

Dalian University of Technology, China

Environmental & Water Resources Engineering Ltd., Israel

ICL, UK

Institut National de l'Environnement Industriel et des Risques, France

Demokritos, National Research Centre for Physical Sciences, Greece

Onderzoekscentrum voor Aanwending van Staal, Belgium

University of Leeds, UK

CanmetENERGY, Canada

One Dimensional Impure CO_2 Plume Migration in a Storage Reservoir and its Geochemical Impact on Mineral Alteration

J. L. Wolf and D. Rebscher

Federal Institute for Geosciences and Natural Resources (BGR), Department of Subsurface Use, Geological CO_2 Storage, Hannover, Germany

Work package 3 (WP3) embedded in the CO_2QUEST project investigates the effects of impurities on the performance of geological storage of carbon dioxide. A prominent part of this work is to identify and study critical processes during CO_2 storage in terms of geochemical disturbance and mineral alteration of the reservoir rock and brine system in a deep saline storage aquifer.

One of these processes is the migration and spreading of an impure CO_2 plume into the reservoir rock. Here, an important question relates to different aqueous solubilities of impurities compared to CO_2. While chemically inert gases like nitrogen (N_2) or argon (Ar) dissolve into the formation water only to a very small degree, essentially, they will remain in the CO_2 rich phase. In contrast, other impurities like sulphur dioxide (SO_2) evince a far stronger solubility and will partition into the aqueous phase comparatively fast. Therefore, an impurity

enriched aqueous zone emerges close to the injection zone, with rather high impurity concentrations resulting in an increased chemical reactivity. However, this partitioning ambition of SO_2 and its subsequent spatial distribution depends on a variety of initial and local parameters, such as porosity, permeability, pressure, temperature, salinity, injection rate, and chemical conditions.

In WP3, numerical reactive transport simulations were performed using the recently released code TOUGHREACT V3.0-OMP (Xu et al., 2014). At BGR, we developed two computational model approaches for the reacting sulphur chemistry. One approach accounts for fast reactivity (SO_2aq equilibrium speciation), the other for slow reactivity (SO_2aq kinetic speciation) influencing the total SO_2 solubility and the spatial extent of the dissolution. The general 1D-radial grid model is based on field data from the CCS test site in Heletz, Israel. In order to account for the influence of the most prominent parameters on the quantitative numerical results, single values were varied within realistic ranges and a set of simulations were performed to test the sensitivity of the results in relation to each parameter. The injection period in the simulation lasted ten years with an injection rate of 1.8 kg/s of 99 % CO_2 and 1 % SO_2.

The numerical results at the end of the injection period are shown in Figures 1 and 2. The CO_2 plume itself extends to 1500 m in the lateral
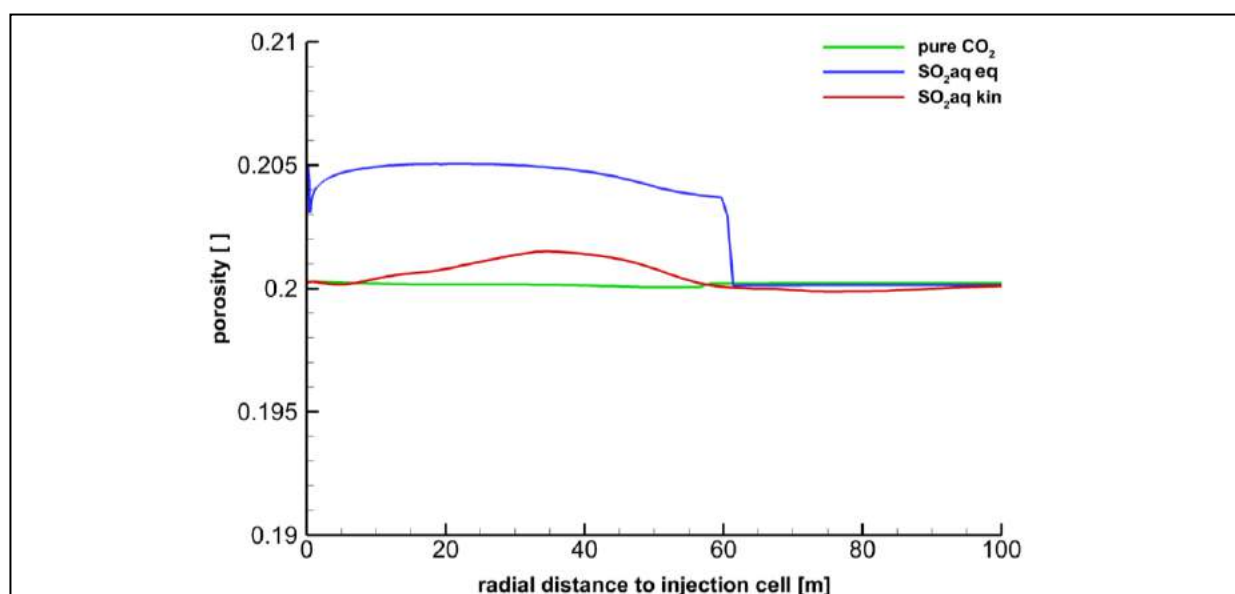

Figure 1. Overall SO_2 induced porosity profile computed with two different reacting models. The fast equilibrium SO_2aq eq is shown in blue and the slow kinetic reaction SO_2aq kin in red after co-injecting CO_2 and SO_2 for 10 years with a rate of 1.8 kg/s. In comparison, the green line indicates alterations in the case of pure CO_2 injection.
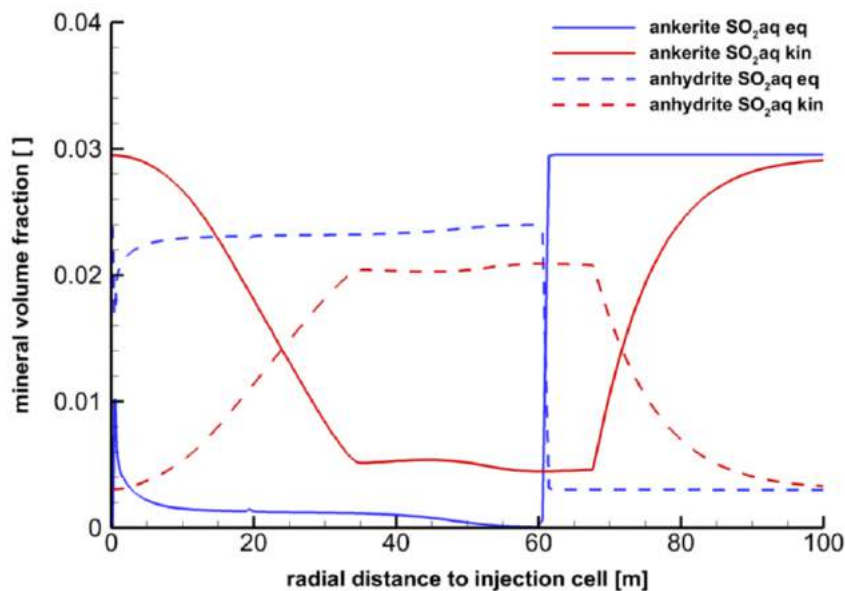
Figure 2. Spatial profiles of the calcium-bearing minerals ankerite and anhydrite resulting from SO_2 induced transformation of carbonate to sulphate. Simulations using equilibrium influence the region around the injection with a spatial extent of 60 m. In the kinetic approach, the region where these chemical alterations take place is more spread out due to transport. Hence, changes can be detected up to distances to the injection site of about 100 m. Results are shown after the co-injection of 1.8 kg/s CO_2 and SO_2 for 10 years.

extent (not shown), whereas the SO_2 impurity dissolves within the first 60 m to 100 m, depending on the chosen model. The difference in the spatial distribution of the dissolution is due to blurring effect of transport. The dissimilarity of the two models can be seen in the overall porosity change due to the chemical impact of the SO_2 impurity on the minerals (Figure 1). After SO_2 oxidation or disproportionation to sulphuric acid, the dissolved SO_2 reacts with the available pH sensitive carbonate mineral ankerite ($CaFe(CO_3)_2$.), which is directly transformed into the sulphate precipitate anhydrite ($CaSO_4$). This is apparent in the almost horizontal flip of the spatial profiles of ankerite and anhydrite (Figure 2). The overall porosity change, which in this case relies mainly on the ankerite-anhydrite interplay, is one important parameter in regard to the study of an adequate storage performance. Based on results obtained by these sets of simulations, a more sophisticated model for 2D simulations on reservoir scale for impure CO_2 storage will be developed.

References

Xu, T., Sonnenthal, E., Spycher, N., and Zheng, L., TOUGHREACT V3.0-OMP Reference Manual: A Parallel Simulation Program for Non-Isothermal Multiphase Geochemical Reactive Transport, Lawrence Berkeley National Laboratory Report LBNL-Draft, Berkeley, California, pp141, 2014.

An Introduction to CanmetENERGY

C. Salvador, K.E. Zanganeh and A. Beigzadeh

Natural Resources Canada, CanmetENERGY, Canada

Natural Resources Canada's CanmetENERGY is the Canadian leader in clean energy research and technology development. With over 450 scientists, engineers and technicians and more than 100 years of experience, CanmetENERGY is Canada's knowledge centre for scientific expertise on clean energy technologies. It is the largest energy science and technology organization working on clean energy research, development, demonstration and deployment. The goal is to ensure that Canada is at the leading edge of clean energy technologies to reduce air and greenhouse gas emissions and improve the health of Canadians. CanmetENERGY manages science and technology programs and services, supports the development of energy policy, codes and regulations, acts as a window to federal financing and works to develop more energy efficient and cleaner technologies.

Within the context of the CO_2QUEST project, CanmetENERGY is conducting experimental studies to provide data on the thermos-physical properties of CO_2 mixtures over a range of pressures and temperatures, and the effect of CO_2 mixtures containing impurities on pipeline materials and reservoir cap rock specimens.

VLE & Transport Properties Measurement

With respect to the work on the thermo-physical properties of CO_2 mixtures, CanmetENERGY's work directly supports the effort under CO_2QUEST for developing more accurate equations of state (EOS) for these mixtures. Unfortunately, there is an absence of data for CO_2 mixtures, particularly for quaternary and tertiary mixtures, at the pressure and temperatures typical of CCS processes in the open literature, forcing modellers to use more generic EOS to make predictions about the thermo-physical properties of CO_2 mixtures. Thus, by working closely within the CO_2QUEST's partners, CanmetENERGY is conducting experiments to generate data and fill some of the gaps in the available thermos-physical properties of CO_2 mixtures.

In this context, experiments are carried out using a unique bench-scale CO_2 pressure cell apparatus (0 – 200 bar and -60 to 150°C). In brief, the pressure cell assembly consisting of a high pressure view chamber, gas mixing and booster pump assembly, syringe pump, recirculating pump, heating/cooling enclosure, density meter and gas chromatograph (Figure 3).
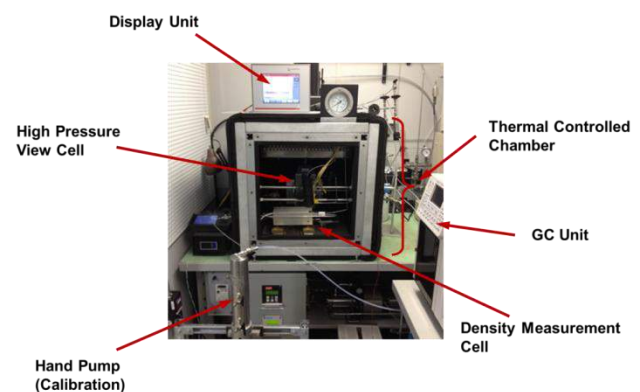

Figure 3. CanmetENERGY's bench-scale CO_2 pressure cell apparatus.

A camera system, situated immediately outside the high pressure view chamber records the phase change of the fluid within the high pressure cell in real time. The novel design for the high pressure view chamber provides the

unique opportunity to observe the phase change visually (Figure 4) ensuring the correct sampling is made from either the liquid or vapour.
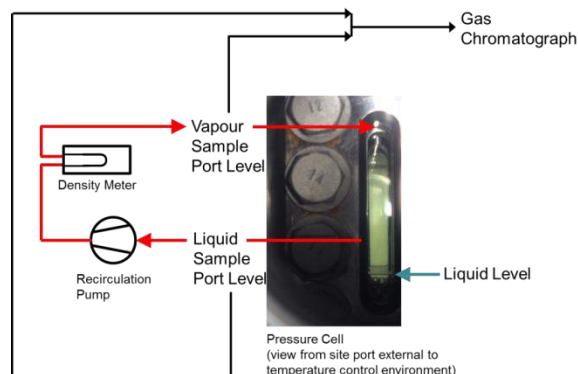

Figure 4. Two phase mixture, as viewed from observation window.

This experimental investigation is focused on the measurement of density and concentration for pressures from 5-80 bar and temperatures from 220-300 K, for a single quaternary mixture and three tertiary mixtures. Testing for the quaternary mixture (CO_2 (93%), O_2 (5.4%), N_2 (1.49%), and Ar (649ppm)) is ongoing with positive preliminary data at 300 K and 280 K, when compared with estimates from HYSYS. A subsequent snapshot of the density data relative to values from HYSYS are shown in Figure 5. Currently work is continuing with testing at 260 K and 240 K, with the tertiary mixtures to follow.
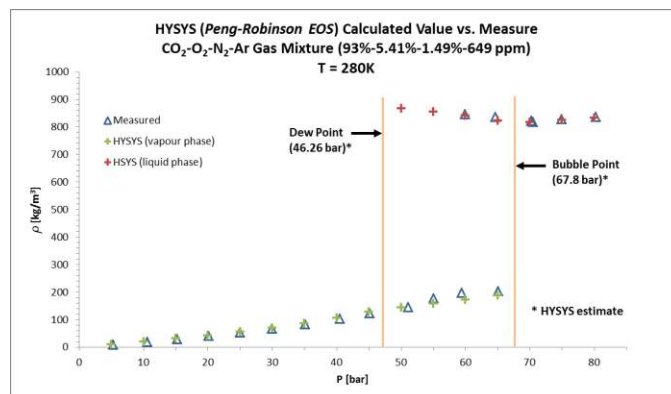

Figure 5. Quaternary gas mixture measured data versus HYSYS calculated values.

Corrosion of Pipeline and Wellbore Materials

Characteristics of CO_2 streams captured from the fossil fuel-fired plants vary depending on the type of fuel, combustion technology, extent of flue gas processing, as well as the CO_2 capture technology used. The captured CO_2 rich flue gases can be categorized into two main categories:

1. Oxidizing CO_2 streams with residual O_2 and SO_2 (e.g. from oxy-coal combustion plants); and,
2. Reducing CO_2 streams with H_2S and almost no residual O_2 (e.g. from coal gasification processes).

The major difference between the two types of captured CO_2 streams are the concentrations of the so-called non-condensable impurities such as O_2, and the reactive reducing or oxidizing agents SO_x or H_2S impurities, as well as residual quantities of H_2O and HCs in these streams. In the presence of H_2O the main factor affecting the corrosion rate may be related to pH change or gas-chemical reactivity forming acidic condensates for example, on wetted steel surfaces. Commonly, flue gas processing and compression systems involve dehydration step(s) which reduce the downstream corrosion

caused by formation of acidic condensates. Corrosion and impact of impurities are also of concern in the CO_2 injection and storage sites. The downhole tubular (consisting of steel casing pipe to secure the hole) used for injection, is secured by cementing to avoid contamination from other underground fluids. Therefore, it is important to study the behaviour of steels used in wellbores in the presence of the aforementioned supercritical CO_2 mixtures at typical well temperatures, pressures, and flow conditions.

The work on materials corrosion is done in collaboration with researchers at CanmetMATERIALS and aims to quantify the extent to which supercritical CO_2 mixtures, containing the impurities O_2, H_2O, H_2S or SO_2, interacts with steels typical of pipeline transportation and wellbore casings, through experimental studies. In order to mimic pipeline transport and injection temperature, pressure and flow conditions, a temperature-controlled autoclave with a rotating cage containing coupons of materials to be tested is employed (Figure 6). Three candidate pipelines and wellbore carbon steels, namely, X65, X70, and X80 are being tested to determine the nature and rate of corrosion for these materials in the presence of supercritical CO_2 with the aforementioned impurities. Standard ASTM methods are employed to accurately quantify and characterize the corroded sample coupons,

which are exposed to these supercritical CO_2 mixtures for a predetermined 120 hour period. Furthermore, state-of-the-art electron microscopy techniques are employed for post-mortem examination of the coupon surfaces, such as Scanning Electron Microscopy and Energy Dispersive X-ray spectroscopy (SEM/EDX), transmission electron microscopy (TEM).
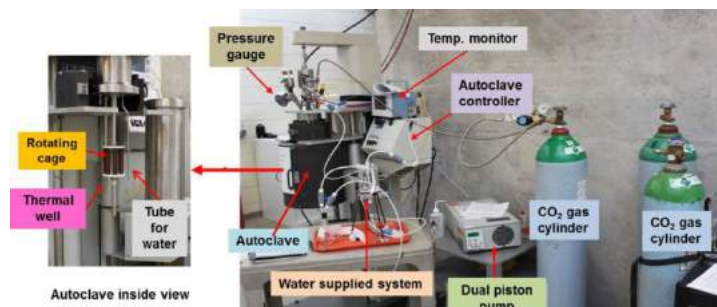

Figure 6. Experimental apparatus employed at CanmetMATERIALS for corrosion testing of candidate steels.

A summary of preliminary test results are provided in Table 1, specifically the average corrosion rate for the candidate materials as function of pressure, temperature, and impurities. Figure 7 depicts a sample SEM/EDX analyses performed on X80 for test condition #3, which shows a porous rust layer was uniformly grown on the steel surface after the test, and that the corrosion layer contained different types of iron oxides.

Test ID	Test Conditions					Average Corrosion Rate (µm/yr)		
	Pressure (psig)	Temp (C)	Impurities (Vol %)	Duration (hours)	Rotation Speed (rpm)	X65	X70	X80
#1	1450	45	CO2+Sat. H2O	120	100			12.2
#2	1520	45	CO2+Sat. H2O+3% O2	120	100	33.2	32.9	41.6
#3	1510	45	CO2+Sat. H2O+3% O2	120	500	102.3		89.8
#4	1480	45	CO2+Sat. H2O+6% O2	120	100	83.2		71.8

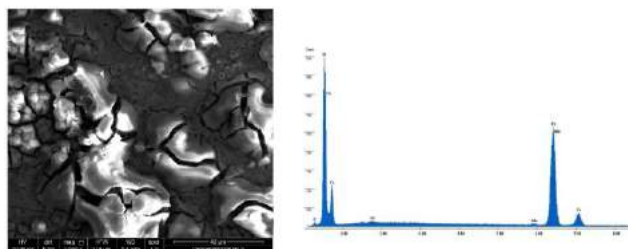**Table 1.** Summary of preliminary corrosion rate results.

Figure 7. SEM image and EDX analyses recorded on an X80 steel coupon after Test#3.

Furthermore Figure 8 shows the results of TEM which shows that the formed corrosion layer for X80 exposed to test condition #1 is composed of $Fe(CO_3)_2$ and some iron oxides. At present, these candidate materials are undergoing further testing over a range of pressures and temperatures while being exposed to different concentrations of impurities for evaluation of the corrosion rate, in addition to surface corrosion characterization via scanning electron microscopy.
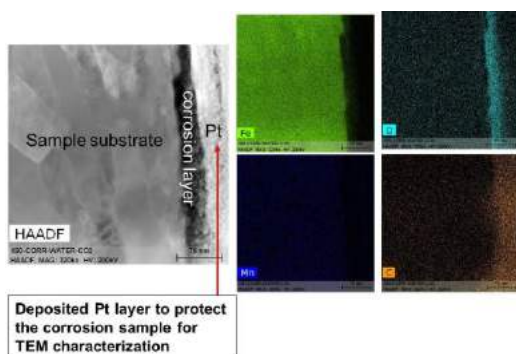

Figure 8. TEM characterization of X80 sample after Test #1.

Experimental Evaluation of Impurities Effects on Storage

Similar to the corrosion work sighted above, CanmetENERGY's Subsurface Environment Group is investigating the impact of impurities on reservoir and caprock sandstone samples from Heletz reservoir in Israel in order to determine if the proposed impure CO_2 stream containing 2% SO_2 may result in unwanted deleterious impacts to injectivity and storage security. Reservoir samples are currently being tested at reservoir conditions in high pressure and temperature reactors (see Figure 9) in which they are exposed to synthesized formation brine and pure and impure CO_2 streams. Changes to the geochemistry of the fluid and mineralogy will be used to infer impacts to the reservoir. Caprock testing will be initiated shortly and will involve measuring a suite of geomechanical properties, including tensile strength and radial permeability, of samples that have been soaked in brine saturated with pure and impure CO_2, as well as unconditioned samples, in order to determine the impact of the impure CO_2 stream on caprock integrity.

Figure 9. CanmetENERGY's high pressure and temperature reaction vessel test setup.

Industrial Scale CO2 Release Experiment - Dense CO2 Release

S. Chen, Y. Zhang, Y. Jianliang and X. Guo

School of Chemical Engineering, Dalian University of Technology, China

DUT so far has performed many all types of CO_2 release experiments including gaseous, supercritical and dense liquid releases, using the 256 m long, 233 mm i.d. pipeline. Recently, a dense CO_2 release was successfully performed with an inventory of 9 tons of liquid CO_2 in the 11 m^3 pipeline (90 bar, 10 degree centigrade, 50 mm orifice).

Figure 10 to Figure 12 show the pressure and temperature change during the dense CO_2 release experiment. It can be seen that the pressure dramatically decreased from 90 bar to 40 bar (near saturation) as soon as the release was triggered. Temperature of the fluid near release point varied regularly, however it changed violently near the closed end and the temperature was much lower than the other positions far away from the closed end. The temperature change of the pipeline wall however is opposite to that of the fluid in the pipeline. The temperature of the wall near the release point is much lower than the closed end. Dense Full Bore rupture CO_2 release is being under preparation.
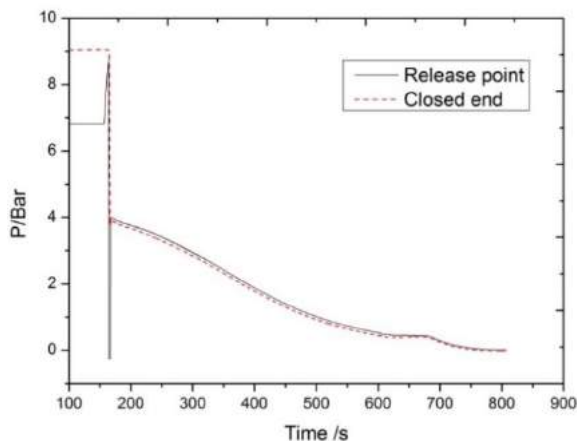

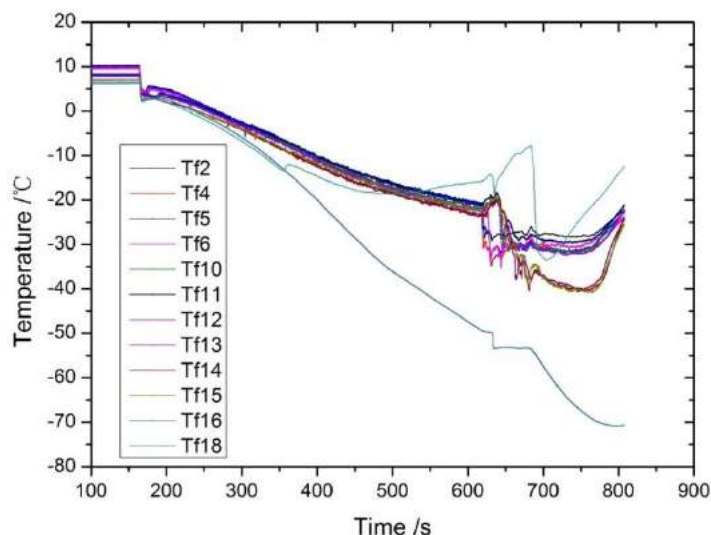**Figure 10.** Depressurization of the pipeline during dense CO_2 release.

Figure 11. Temperature change of the CO_2 fluid in the pipeline during the dense CO_2 release.
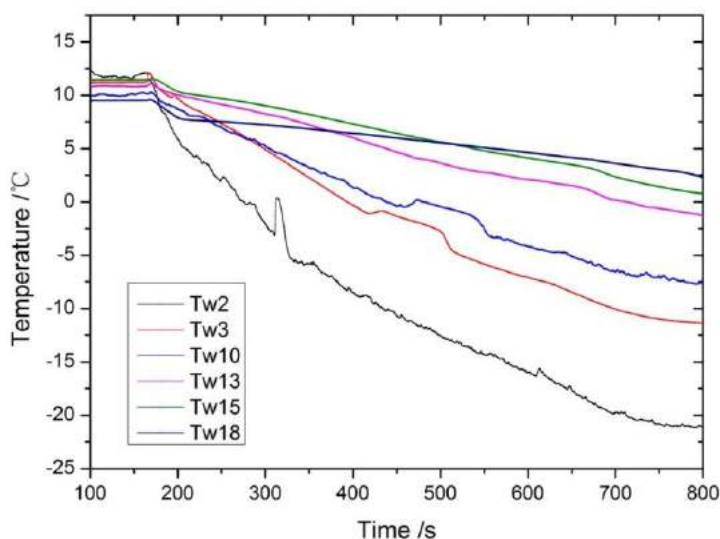

Figure 12. Temperature change of pipeline wall during the dense CO_2 release.

Figure 13. Photograph of dispersion cloud formed in the dense-phase CO_2 release test.

8

Figure 14. The photograph of the release jet at the late stage of a pipeline decompression test.

In order to quantify the impact of impurities on the CO_2 dispersion, several puncture release tests have been performed for CO_2 mixtures with nitrogen. In these tests the detailed information about the flow, temperature and concentration of the released CO_2 plume have been obtained, which is essential for validation of computational CO_2 dispersion models.

The Impact of Impurities on Storage

J. Bensabat and R. Segev

EWRE Ltd., Haifa, Israel

Design of the Impurities Injection System

We have completed the fine design of the impurities injection system for N_2 and SO_2, trying to make maximum use of the available infrastructure (High pressure N_2 booster and supply line). The design of the SO_2 injection line was rather complex.

Regulatory Issues, Health, Safety and Environment (HSE)

A permit for the temporary storage of SO_2 on site (during the injection) had to be obtained from the Ministry for the protection of the environment, which required permits from a number of other authorities (fire department, the home front command etc.). A permit for the injection of SO_2 in the CO_2 stream was also filed to the Israel Water Authority. A HSE plan was prepared, in order to put on site mitigation measures, subsequent to possible accidents during the storage and or the injection of SO_2, even for a very short period of time.

Hazard and Operability Study – HAZOP

This activity investigates the possible failures than can occur during the storage and or injection of SO_2 and determines measures to prevent them (via some redundancies in the equipment and / or mitigation measures should an incident occur). This study has been completed.

Towards Injection

The injection system is under commissioning, checking the safety and operability of every one of its components. This process should be completed by the end of August, 2015. After the completion of the commissioning we shall start the injection of pure CO_2 and after this experiment we shall engage in the injection of the CO_2 + impurities.
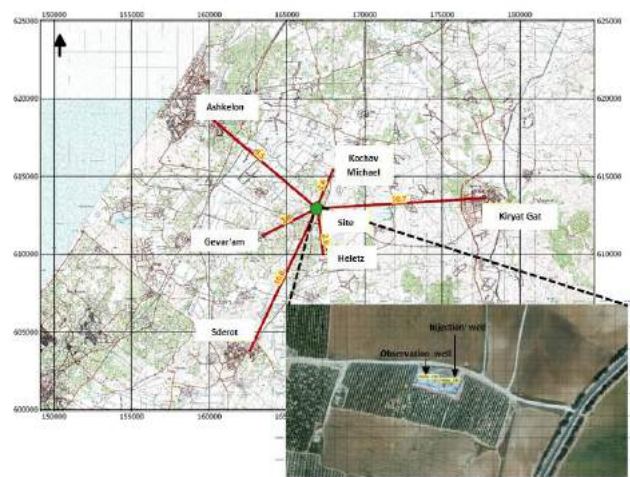

Figure 15. Aerial distance map of the site and the closest towns, including an inset showing an aerial photograph of the site.
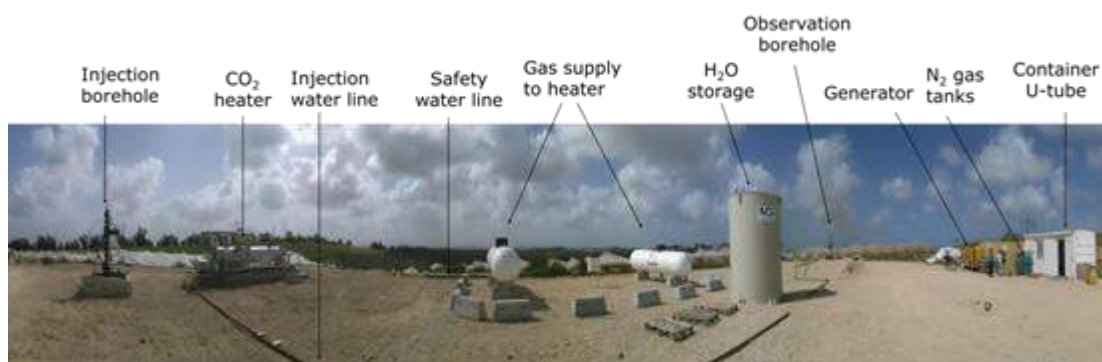

Figure 16. Photograph of impurities injection system.

A Techno-economic Analysis of Gas Purification and Compression for CO_2 Capture, Shared Capture Infrastructure and CO_2 Transport Networks

C. Kolster, E. Mechleri, S. Krevor and N. Mac Dowell

Imperial College London, UK

CO_2 Compression and Purification Units

Oxy-combustion capture is currently one of the most promising methods of CO_2 capture as it is one of the most developed and technologically mature for Carbon Capture and Storage (CCS). Unlike other mature technologies, oxy-combustion capture presents a trade-off between cost and purity. Oxy-combustion capture consists of an air separation unit (ASU) that produces a high purity oxygen stream and, mixed with recycled flue gas, provides a high-oxy environment in which to burn the fuel. The flue gas produced by oxy-fuel combustion will vary in purity, depending on the input conditions, and still requires dehydration, further purification and compression in order to be suitable for transport and storage. The latter is performed by means of a CO_2 Compression and Purification Unit (CO_2CPU). The process is represented in Figure 17.
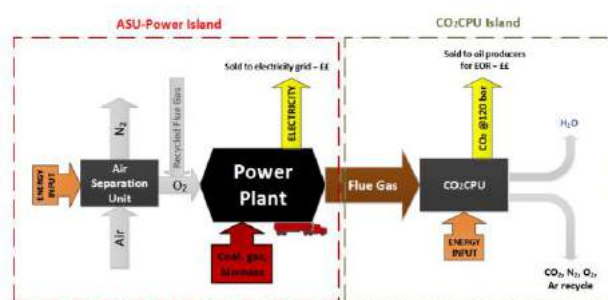

Figure 17. Illustrative diagram of the oxy-combustion capture process highlighting the main energy intensive units and revenue sources and outputs for each island: the ASU island and the CO_2CPU island.

In this work we have modeled four variations of the CO_2CPU in Aspen HYSYS using a Peng-Robinson property method with each system varying in their method of separation. These models were based on similar models presented by Posch et al. (Posch S.). The four models in order of descending complexity are: a CO_2CPU

with a 6-stage distillation column, one with a double flash system with heat integration, one without heat integration and the least complex with only compression and dehydration. The results from these models show that an increase in product purity and complexity results in a reduction in capture efficiency. The capital and operational cost results for each CO_2CPU modeled were translated into a price for the CO_2 product stream shown in Figure 18. In order to derive a price for each product, it was assumed that the CO_2CPU is an independent entity in which to invest, with two inlet streams - raw flue gas (free) and energy (cost) - and two outlet streams - CO_2 product (revenue) and waste stream. Figure 18 shows that at four different minimum rates of return (equated to the internal rate of return IRR), we find a non-linear and non-monotonic relationship between CO_2 price and purity.
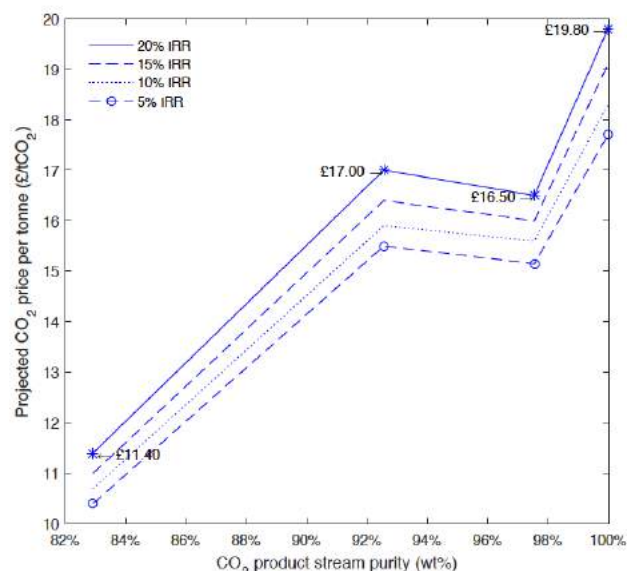

Figure 18. Graph showing the CO_2 price per tonne sold if marketed assuming a minimum rate of return on investment of 20%, 15%, 10% and 5% on the CO_2CPU as a function of CO_2 stream purity.

The difference between the highest purity product at 99.98 wt.% CO_2 and the lowest purity product at 82.91 wt.% CO_2 represents a 42% reduction in price.

CO_2 Transport Networks

Certain considerations must be taken however in terms of the product purity. A large presence of non-condensable gases can reduce storage capacity and also require larger pipeline diameter for an equivalent amount of pure CO_2 at a given pressure. Typically it is recommended to have a purity level for CO_2 of 96% (de Visser E.). Nevertheless, if a combination of cheaper, low

purity sources of CO_2 were mixed with higher purity sources of CO_2 in a transport network system, a final trunk line with a CO_2 stream of composition suitable for injection could be achieved. This concept is illustrated in Figure 19. In order to describe this kind of system we have taken a UK based case study with 10 gas CCGT plants, 10 coal fired plants and one steel industrial plant set up by Prado et al. (Prada, Konda and Shah). Each CCGT plant was assumed to adopt amine-based post combustion capture while the coal plant and steel plant adopt oxy-combustion capture, choosing from one of the oxy-combustion CO_2CPU models described. This scenario was formulated into a bi-objective optimization problem, in GAMS, looking at the trade-offs between optimizing for lowest cost and highest purity. Binary variables of values 0 and 1 were used to represent the choice of CO_2CPU. Figure 20 shows the Pareto front for the competing objective functions: minimum cost and maximum purity assuming a lower bound for CO_2 purity at the trunk line of 96 wt.%. The results in Figure 20 show the average capital and operational costs per tonne of CO_2 captured for the CO_2CPU applied to both post combustion and oxy-combustion capture. The difference between the capital cost for a minimum purity system and the maximum purity system per tonne of CO_2 capture is 45%. Applying the same assumptions as earlier for the CO_2 price, this difference represents a 17% increase in CO_2 price.
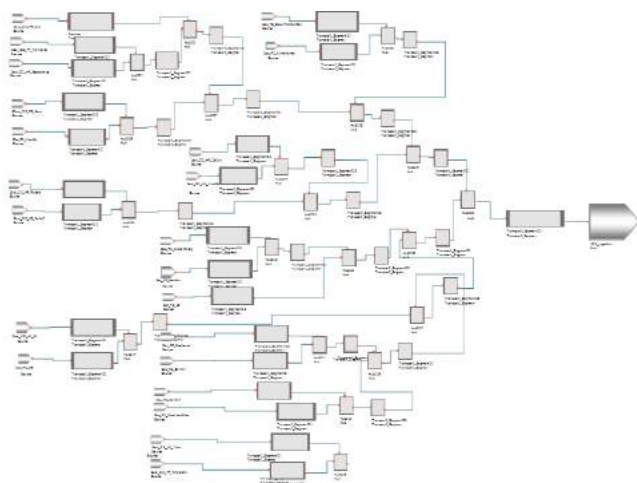

Figure 19. Illustration of a CO_2 transport network case study with 10 CO_2 streams from post-combustion gas CCGT plants, 10 from oxy-combustion coal-fired plants and 1 steel plant with oxy-combustion CO_2 capture feeding into one final CO_2 trunk line.

Shared Capture Plant Infrastructure

With the objective of further reducing the costs of oxy-combustion capture we have studied the financial benefits of having a shared CO_2 compression and purification unit with a throughput of 20 Mt CO_2/year (equivalent to the output of a large power plant such as Drax) as opposed to having four CO_2CPUs each with a throughput of 5Mt/year.
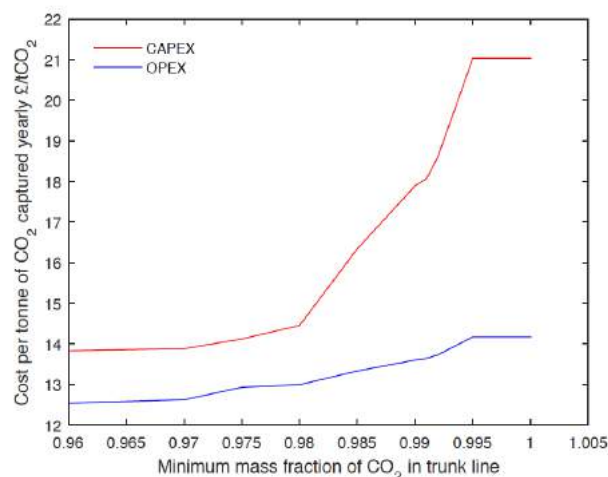

Figure 20. Graph showing the network capture system CAPEX and OPEX per tonne of CO_2 captured yearly as a function of minimum trunk line purity – optimization problem Pareto front.

In this study we do not include transport costs, however, these are deemed to be significantly lower than capture costs: onshore pipelines are 25-30 times less cost intensive per tonne of CO_2 than the cost of capturing (Prada, Konda and Shah). The results of this study show that having one large 20Mt CO_2/year plant reduces the total capital expenditure by 16% and the yearly operating expenses by 4% compared to having four 5Mt CO_2/year units (see Figure 21). Hence, we can conclude that adopting shared CO_2 capture infrastructure helps reduce the investment risk of CCS.
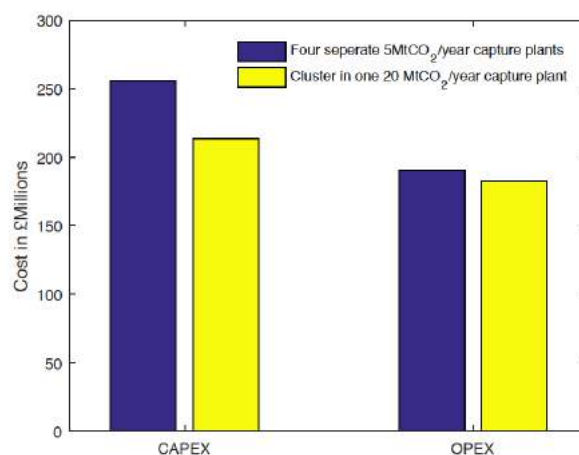

Figure 21. Bar chart showing the CAPEX and OPEX for one large CO_2CPU processing 20 $MtCO_2$/year compared with four CO_2CPU plants each with a 5$MtCO_2$/year throughput.

Cost Analysis Based on Producing Different Levels of CO_2 Stream Impurities

M. Fairweather[1], C. Kolster[2], N. MacDowell[2], R.T.J. Porter[1†], N. Shah[2] and R.M. Woolley[1]

[1]*University of Leeds, UK*

[2]*Imperial College London, UK*

[†]*Currently: University College London, UK*

The University of Leeds and Imperial College London have collaborated on a study to analyse the trade-off between the cost of carbon capture and the purity of the product CO_2 stream from coal-fired power sector CCS plants. Techno-economic modelling approaches have been used to calculate various performance factors and costs of CCS plants. The three main types of power sector CCS plants of oxyfuel combustion, pre-combustion and post-combustion capture with different process scenarios were considered and the impact on cost and product composition of CO_2 was assessed.

Oxyfuel Combustion Capture

In modelling oxyfuel combustion capture plants, Aspen HYSIS was used to undertake detailed simulation of the CO_2 Compression and Purification Unit (CPU) section of the plant which can deal with the removal of non-condensable components of N_2, O_2 and Ar, and compression of the product stream to high pressures (> 100 bar). Based on the same composition and flow rate of raw oxyfuel CO_2 flue gas, three different compression and purification process strategies were considered:

1) CO_2 compression and dehydration only

2) 'Double flash' purification system
3) Distillation purification system

In all cases, the CO_2 product pressure is 120 bar. The first case of CO_2 compression and dehydration only, consists of a 3-stage compression train with interstage cooling and flash separation, followed by a dehydration step and a final 3-stage compression train with interstage cooling to the final delivery pressure. In the second double flash case, a 3-stage compression train with interstage cooling and flash separation followed by a dehydration step is again used. Following this, the flue gas is cooled to low temperatures in 2 multi-stream heat exchangers which are each followed by flash separation vessels. A CO_2 rich liquid stream exits the bottom of the flash separation vessels and a non-condensable gas stream exits the top. Cooling for the multi-stream heat exchangers is provided by auto-refrigeration expansion of the CO_2 product stream. The product stream is compressed further in a 3-stage compression train with interstage cooling. The third distillation case is similar to the double flash case but with phase separation handled by a 6-stage distillation column instead of the double flash vessel system.

Important parametric information results from the oxyfuel compression and purification scenario analysis, including the CPU's total capital and operating costs calculated through Aspen cost functions, the product stream composition and the CPU energy requirement (in kWh/tonne of CO_2 captured). This information is used to calculate the impact of the different CO_2 compression and purification strategies on the overall power plant costs using the Integrated Environmental Control Model (IECM) developed by Carnegie Melon University for typical plants that produce a similar flowrate and composition of raw oxyfuel CO_2 flue gas.
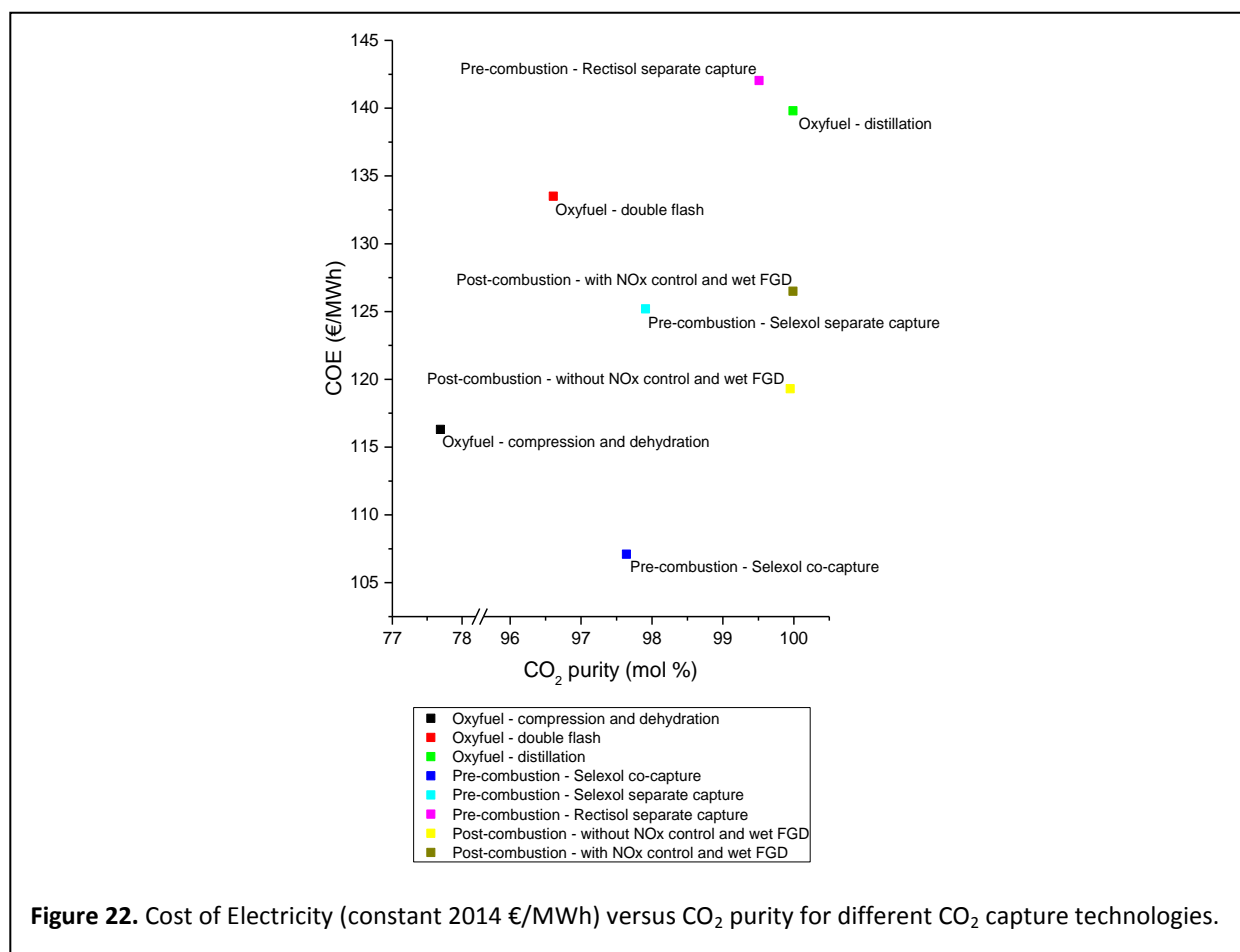
Pre-combustion Capture

In pre-combustion capture, physical solvents are used to remove CO_2 and H_2S from water gas shifted syngas. In the co-capture configuration, CO_2 and H_2S are removed together in the same product stream, whereas in the separate capture configuration, CO_2 and H_2S are removed in separate streams and the H_2S is processed to a more easily handleable form (e.g. to elemental sulfur in Claus / Beavon-Stretford plants). Furthermore, different solvents have been proposed for pre-combustion capture with different performance and cost impacts. In the present study, the impact of the use of two solvents of Selexol™ and Rectisol® on plant performance, cost and CO_2 purity is assessed for separate capture scenarios. The impact of using Selexol™ in the co-capture configuration is also assessed. To do this, cost and performance models for each process scenario were developed, using a Selexol™ separate capture case in IECM as a starting point and necessary assumptions and literature values for the other cases.

Post-combustion Capture

The cost and performance of plants fitted with post-combustion capture technology using monoethanolamine (MEA) solvent as the CO_2 capture medium were assessed. These plants are assumed to be similar in size to and use the same coal as the oxyfuel combustion and pre-combustion power plants. Two different scenarios were investigated within the IECM framework. The first consists of a plant equipped with pollution control devices of Electrostatic Precipitator (ESP) particulate control system, In-furnace NOx controls, hot-side Selective Catalytic Reduction (SCR) and wet Flue Gas Desulfurisation (FGD) SO_2 control. The second plant is only equipped with an ESP particle control system and therefore supplies a flue gas with higher quantities of impurities to the post-combustion CO_2 capture plant.

Figure 22. Cost of Electricity (constant 2014 €/MWh) versus CO_2 purity for different CO_2 capture technologies.

Results and Conclusions

Altogether, 8 different scenarios were analysed (3 for oxyfuel combustion capture, 3 for pre-combustion capture and 2 for post-combustion capture). The results of the analysis are summarised in Figure 22 which shows the levelised Cost of Electricity (COE) plotted against the final product CO_2 purity.

The technology with the lowest COE is pre-combustion capture using Selexol physical solvent with co-capture of impurities. This technology produces CO_2 with and estimated purity of 97.64 mol% but high estimated levels of H_2S (at 3974 ppm_v). Conversley, the highest cost technology in this analysis is found to be pre-combustion capture using Rectisol solvent and with separate capture of sulfur impurities. The CO_2 stream produced by this technology is dry with low levels of other contaminants such as CO and H_2. The technologies that produce the highest grade of CO_2 are post-combustion capture with NOx and wet FGD environmental control and oxyfuel combustion plant with CO_2 purification by distillation, both producing 99.99 mol% CO_2 product, but with post-combustion capture by lowest cost. The three analysed oxyfuel combustion capture technologies produce the widest range of CO_2 purity with the compression and dehydration only system, that doesn't include any additional purification of the raw CO_2 flue gas stream producing the lowest grade CO_2 stream that contains 77.69 mol% CO_2 and high levels of non-condensable species (O_2, N_2 and Ar) plus acid gas species. The present study should facilitate further analysis of whole CCS chain techno-economics and process configuration.

SAFT EoS Development for Modelling CO₂ Mixtures with Impurities of Interest to CCS Including Fluid-fluid and Fluid-solid Equilibria

I. Nikolaidis, L. Peristeras, G. Boulougouris, D.M. Tsangaris and I. Economou

National Centre for Scientific Research Demokritos (NCSRD), Greece

Recently, we have developed and implemented in Physical Properties Library (PPL), new and robust algorithms for the calculation of phase equilibrium of pure components and multicomponent mixtures. The new algorithms are capable of handling the calculation of:

a) Two phase solid – fluid (solid – liquid, solid – vapor) equilibrium of pure CO_2 and also binary, ternary and multicomponent CO_2 mixtures where carbon dioxide forms the solid phase.
b) Three phase solid – liquid – vapor (SLV) equilibrium of binary mixtures of CO_2.
c) Constant composition vapor – liquid (VLE) phase envelopes of binary and multicomponent mixtures, including the critical region.

For the calculation of two phase and three phase equilibria, where CO_2 forms a solid phase, three different solid models of variable complexity have been coupled with cubic (SRK, PR) and higher order (SAFT, PC-SAFT) fluid equations of state. Moreover, solution algorithms, suitable for every model have been developed for the cases of two phase and three phase equilibrium, respectively. The accuracy of all the corresponding solid models developed, has been assessed using available experimental data of pure CO_2 at solid – liquid and solid – vapor equilibrium conditions. To assess the accuracy of the solid models regarding mixtures of CO_2 with other components of interest to CCS processes and pipeline transportation, the calculations were compared to experimental SLV equilibrium data available in the literature. In Figure 23, the performance of all the solid models against SLV data of CO_2 – N_2 mixture is demonstrated. Of all the models developed in this work, Jager – PCSAFT describes best the experimental SLV data.

To calculate the constant composition (isopleth) vapor – liquid (VLE) phase envelopes of binary and multicomponent CO_2 mixtures, new and robust algorithms have been implemented in PPL. The traditional methods that are utilized to calculate the bubble and dew lines of binary and multicomponent mixtures are not sufficient to
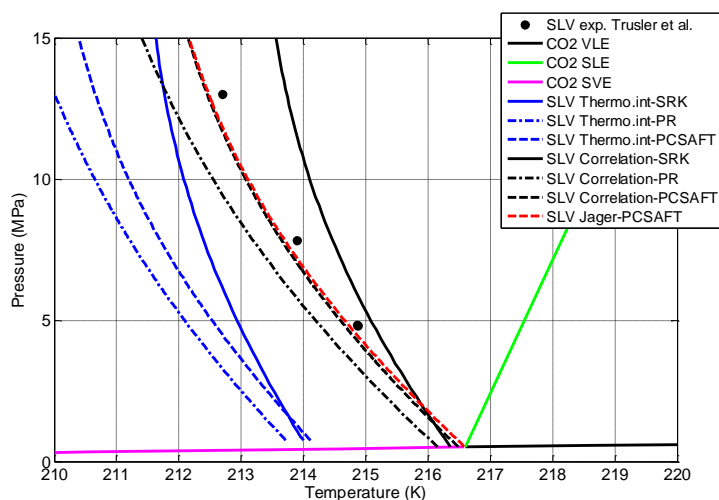

Figure 23. Pressure-Temperature Solid - Liquid - Vapor equilibrium curves for a CO_2 – N_2 mixture. Comparison between Experimental data and different EOS.

calculate the complete VLE phase envelopes, because the retrograde behavior of these mixtures and the presence of critical points cause significant numerical difficulties which result into divergence and subsequent crash of the code. The new algorithms are capable of sequentially tracing the complete isopleths by utilizing compositional derivatives calculated from the equation of state (EoS) and by using accurate initial estimates. This way, the entire retrograde region can be calculated and also the critical point can be bypassed. The new algorithms have been applied to cubic (SRK, PR) and also higher order (SAFT, PC-SAFT) equations of state. In Figure 24, constant composition phase envelopes of different CO_2 mixtures calculated with different equations of state are depicted.

Integration of Physical Properties Library (PPL) with CFD and outflow Computer Codes

A new Physical Properties Library version has been released which includes major computer code restructuring aiming to:

- Improve code maintainability
- Improve extensibility of the software with respect to the integration of new schemes for thermodynamic modeling and their application to an extended set of systems and components
- Increase usability through establishment of a distribution protocol

The new version of the computer code features:

- a source code structure in correspondence with the basic components
- minimum duplicated code
- modular approach
- automated test frameworks capable of testing the basic PPL functionality and verifying the distributed packages
- a modern version control system (git) capable of monitoring and controlling the development and distribution of the software
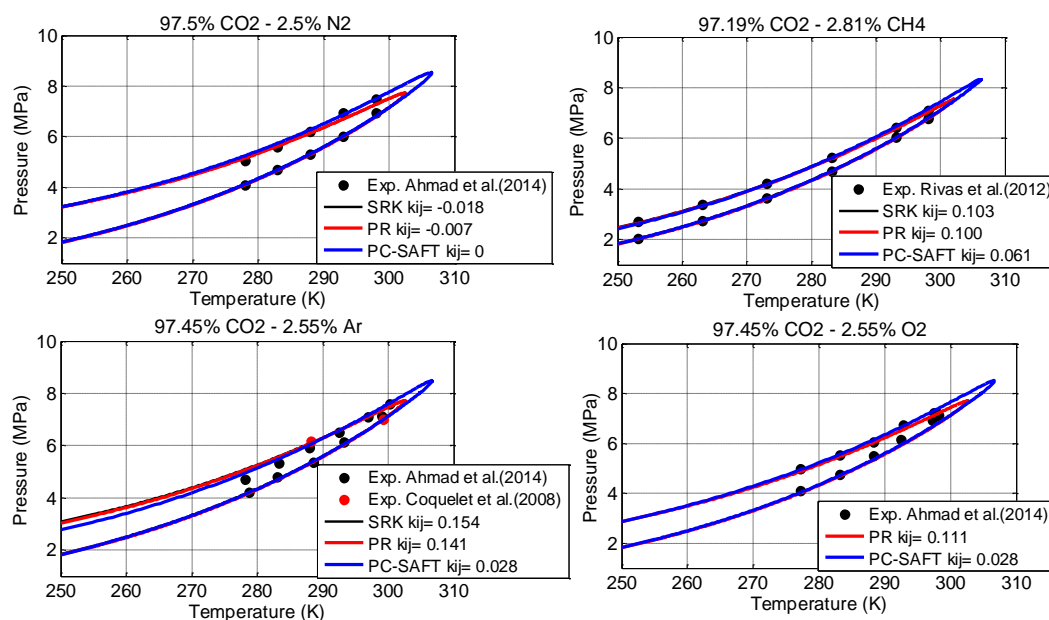

Figure 24. Pressure-Temperature equilibrium curves including the "near critical region" for CO_2 mixtures with N_2, Ar, CH_4 and O_2. Comparison between experimental data and model predictions using different EOS.
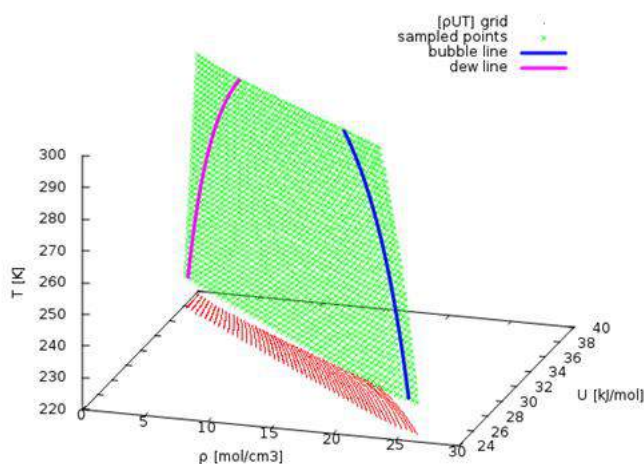
Figure 25. A [ρ, U, P] grid. The red points are the established grid points while the green points are sampled points. The dew (purple) and bubble (blue) lines are also projected on the surface.

With respect to code integration with partner codes, we addressed the problem of avoiding time-consuming thermodynamic calculations during the "computer cycles" of computational fluid dynamics solvers (CFD). Our solution is based on *continued and smooth maps* between thermodynamic properties, such as temperature (T) and pressure (P) and internal energy (U) and density (ρ). After we determine the desired functions, we "map" the properties of interest and finally, use "grids" in order to access these "maps" at runtime. As a result, the computation cost of the thermodynamic calculation diminishes. A short layout of the mapping procedure is the following: for a given *P-T* range, data points connecting a (*T, P*) point with The (U,ρ) point are sampled and used to establish the grids connecting the (ρ, U) points with the pressure ([ρ, U, P] grid) and the temperature ([ρ, U, T] grid) of the system. Notice that, more than one grid can or should be used to model the system in a wide range of conditions required in CO_2QUEST project (i.e. vapor and liquid phase as well as the vapor-liquid and solid-vapor equilibrium regions). In Figure 25, the produced [ρ, U, T] grid for a system with 96% CO_2 and 4% N_2 is demonstrated. Currently, we are working on modelling the solid-vapor equilibrium region as our partners are testing, verifying and extending the existing grid functionality.

References

[1] N.I. Diamantonis and I.G. Economou, "Evaluation of Statistical Associating Fluid Theory (SAFT) and Perturbed Chain-SAFT Equations of State for the Calculation of Thermodynamic Derivative Properties of Fluids Related to Carbon Capture and Sequestration", *Energy & Fuels*, **25**(7), 3334 – 3343 (2011).

[2] N.I. Diamantonis, G.C. Boulougouris, E. Mansoor, D.M. Tsangaris and I.G. Economou, "Evaluation of Cubic, SAFT, and PC-SAFT Equations of State for the Vapor-Liquid Equilibrium Modeling of CO2 Mixtures with Other Gases", *Ind. Eng. Chem. Res.*, **52**(10), 3933 – 3942 (2013).

[3] N.I. Diamantonis, G.C. Boulougouris, D.M. Tsangaris, M.J. El Kadi, H. Saadawi, S. Negahban and I.G. Economou, "Thermodynamic and Transport Property Models for Carbon Capture and Sequestration (CCS) Processes with Emphasis on CO2 Transport*", Chem. Eng. Res. Des.*, **91**(10), 1793 – 1806 (2013).

[4] NIST database: http://webbook.nist.gov.

[5] Ilias K. Nikolaidis, Georgios C. Boulougouris, Dimitrios M. Tsangaris, Loukas D. Peristeras, Ioannis G. Economou, "Modeling solid – fluid equilibria with application to CO2 mixtures", 28th *European Symposium on Applied Thermodynamics*.

Numerical Simulation of Prolonged Release Experiment Using Coupled Fluid-Structure Modelling Approach

R. Hojjati-Talemi[1], S. Cooreman[1], S. Brown[2] and S. Martynov[2]

[1]*ArcellorMittal Global R&D Gent (OCAS N.V.), Belgium*
[2]*University College London, UK*

In the framework of the CO_2QUEST project a coupled fluid-structure fracture model has been developed in cooperation with University College London (UCL). The developed model is validated against a full scale prolonged release experiment from literature.
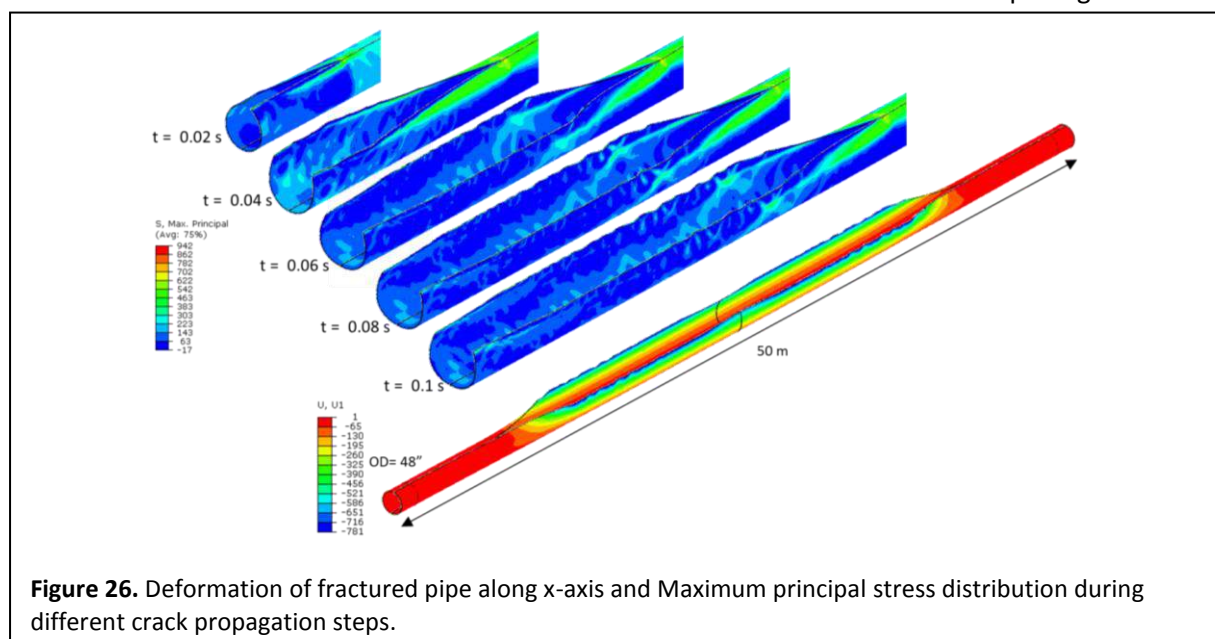
Coupled Fluid-structure Model

The occurrence of a longitudinal crack propagating along a CO_2 pipeline is a catastrophic event, which involves both economic losses and environmental damage. Therefore, the fracture propagation estimation is an essential strategy to ensure pipeline integrity. Fracture prediction is a challenging task, since it requires knowledge of the interaction between the dynamic forces driving crack growth, and the resistance forces opposing fracture propagation. Moreover, plenty of material properties should be taken into account. The coupling of the pipe decompression (CFD outflow), developed by UCL, and the ductile fracture model, developed by OCAS, is based on a feedback algorithm. British Gas Company (BGC) has carried out a series of full-scale burst tests between 1978 and 1983 on 48"x18 mm X70 line pipes with a length of 50 m.

In this study one of these tests was selected for validation of the developed numerical model. The natural gas was pressurized till 11.6MPa. Figure 26 illustrates deformation contour plots of the fractured pipe along with the maximum principle stress distribution during different crack propagation steps up to 0.1 s. From the figure it can be noticed that the ductile crack propagation occurred in a straight line as expected.

In order to model fluid-structure interaction, the first step involved the computations of the bulk fluid pressure and the corresponding crack tip pressure for an arbitrary small initial longitudinal crack opening along the major axis of the pipeline, formed for example, as a result of third party damage. The corresponding crack tip velocity was then calculated using the fracture model. A zero crack velocity meant no propagation and the calculations were terminated. For a positive value on the other hand, the new crack opening area was determined after an arbitrary small time increment (Δt =0.001 s). Based on the new crack opening area and

Figure 26. Deformation of fractured pipe along x-axis and Maximum principal stress distribution during different crack propagation steps.

time interval, the mass of fluid escaping and hence the new crack tip pressure were determined using the fluid flow model. This procedure was repeated for further time increments up to the point in time at which the crack velocity reached zero.

Results and Discussion

Figure 27 shows a detailed view of corrugated deformation of a fractured pipe along the crack propagation path due to plastic deformation. It was realized that this corrugated wave was formed because of the difference between the internal and the backfill pressures at the crack tip position during crack propagation. It can be seen that the predicted results are in good agreement with the experimental observations. Figures 3 (a) and (b) indicate the variation of circumferential stress inside the pipe and flap opening of the fractured pipe at different crack propagation time steps respectively.
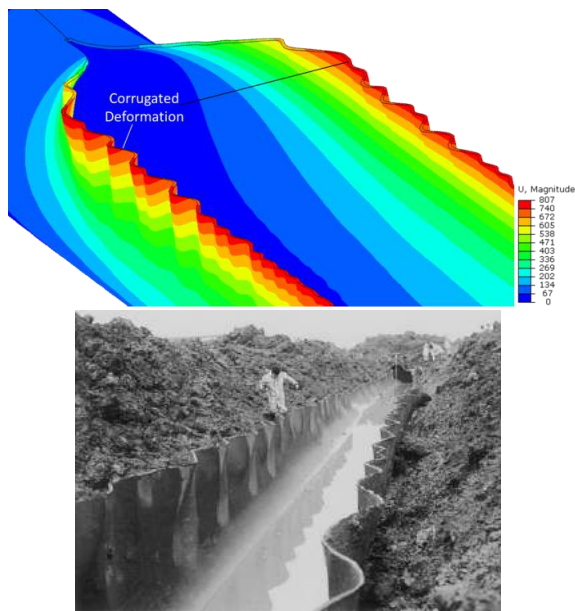

Figure 27. Corrugated deformation along the crack propagation path due to plastic deformation.
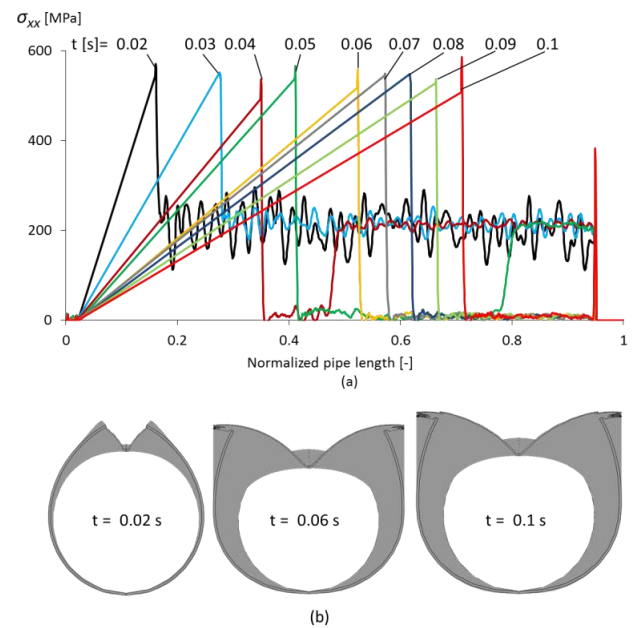

Figure 28. (a) Variation of stress distribution along x-axis inside the fractured pipe and (b) flap opening of fractured pipe during ductile crack propagation steps

Figure 29 depicts a comparison of crack velocity versus crack length between the fluid-structure coupled fracture model (MBW+CFD) considering various number of cells for the CFD code, the High Strength Line Pipe Committee (HLP) method (empirical approach) and experimental observations from literature. As depicted in the figure, for the crack extending from 8 to 20 m, the crack velocities predicted using the coupled model (MBW+CFD) are around 150 m/s and in good agreement with the experimental data.
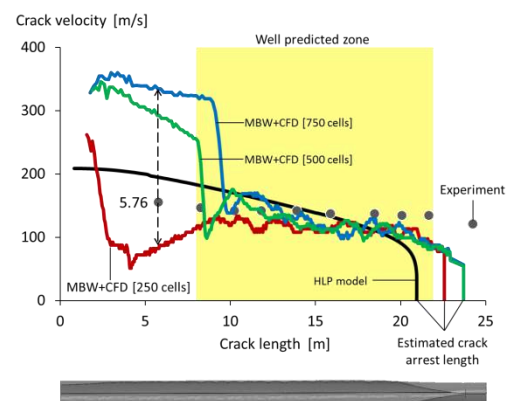

Figure 29. Predicted crack propagation velocity by MBW+CFD and HLP models in comparison with prolonged release experimental observations from literature.

Pipeline Pressure Drop and Compressor Requirements

S. Martynov, S. Brown and H. Mahgerefteh

University College London, UK

It is generally accepted that the use of integrated pipeline transportation networks represents the most practical and economical means of transporting CO_2 streams captured from various emission sources, such as power plants and cement and steel manufacturing industries for long-term geological storage (Knoope et al., 2014). The quality of the CO_2 streams injected into such network will vary depending on the type of fuel and CO_2 capture technology (pre-, post- and oxy-combustion). This represents a practical dilemma given the established impact of the various impurities on many aspects of the CCS performance.

An ability to accurately model the flow within a pipeline network, in particular the pressure drop, fluid phase and precise stream composition including the mixing of the various source streams and the delivery conditions is therefore essential.

In the CO_2QUEST project, the UCL team has developed a computational model for simulation of CO_2 transport in pipeline networks (Brown et al., 2015). This model accounts for all of the pertinent physical phenomena affecting the flow, including real fluid behaviour, heat exchange with the surroundings, the variations in the pipeline elevations as well as periodic changes in the CO_2 emission source mass flow rate.

In the present work the flow model developed is applied to examine impact of CO_2 stream composition and variations in conditions at the source points on the flow along the network and characteristics of CO_2 delivered at the sink points.
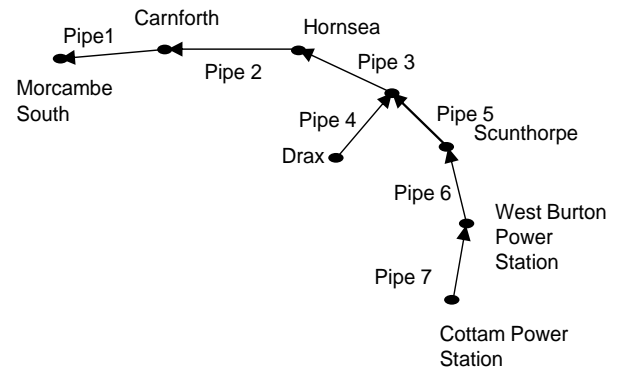

Figure 30. Schematic representation of the pipeline network simulated.

Figure 1 shows configuration of a hypothetical but realistic CCS UK pipeline network, connecting Cottam and West Burton coal power stations in North Yorkshire to Drax power station via Scunthrope steel works. The Drax power station is connected to the main trunk pipeline via a 0.5 km long tie-in line. From this point the CO_2 mixture is transported to its point of sequestration, Morcambe South in the East Irish Sea via Hornsea and Carnforth.

	Scenario 1	Scenario 2	Scenario 3	Scenario 4
Drax composition (vol/vol)	**Post-combustion** $CO_2 - 0.998$ $N_2 - 0.002$	**Oxyfuel** $CO_2 - 0.881$ $H_2O - 0.002$ $Ar - 0.057$ $N_2 - 0.037$ $O_2 - 0.023$	**Oxyfuel** $CO_2 - 0.881$ $H_2O - 0.002$ $Ar - 0.057$ $N_2 - 0.037$ $O_2 - 0.023$	**Post-combustion** $CO_2 - 0.998$ $N_2 - 0.002$
Cottam composition (vol/vol)	**Post-combustion** $CO_2 - 0.998$ $N_2 - 0.002$	**Oxyfuel** $CO_2 - 0.881$ $H_2O - 0.002$ $Ar - 0.057$ $N_2 - 0.037$ $O_2 - 0.023$	**Post-combustion** $CO_2 - 0.998$ $N_2 - 0.002$	**Oxyfuel** $CO_2 - 0.881$ $H_2O - 0.002$ $Ar - 0.057$ $N_2 - 0.037$ $O_2 - 0.023$

Table 2. Compositions of CO_2 streams captured at Drax and Cottam power plants for scenarios 1-4.

Table 1 describes the flowrates and compositions at the source points in four scenarios examined. In all four cases the rate of CO_2 capture at the Drax and Cottam power plants was set respectively to 20.153 Mt/y and 4.847 Mt/y.

Assuming 90 bara pressure at the sink point (Morcambe South), the model developed has been applied to predict steady-state flow field in the network, and in particular the feed inlet pressures and the delivered CO_2 stream composition at the sink point.

Figure 2 shows the predicted pressure profiles along the main trunk pipeline for each of four scenarios from Table 1. As can be seen from Figure 2, in general, an increase in the number of impurities results in an increase in the drop in pressure along the pipeline. Scenarios 1 and 4 produce almost identical pressure profiles despite the fact that the feed composition from Cottam power station is very different in either case. This is due to the much higher feed flowrate from Drax power station (*ca.* 20 Mt y^{-1}) as compared to Cottam power station (*ca.* 4 Mt y^{-1}) thus overshadowing the impact of the latter.
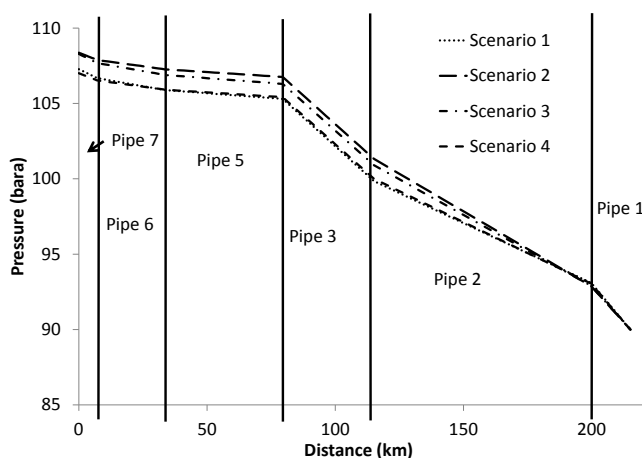

Figure 31. Variation of fluid pressure along main trunk line.

Figure 3 shows the variation of the fluid pressure along the main trunk pipeline for Scenario 3, predicted for the 'normal' as well as 'ramp-up' and 'ramp-down' flowrates respectively. As it may be observed, in general the higher is the flowrate from Drax power station the greater is the predicted pressure drop.
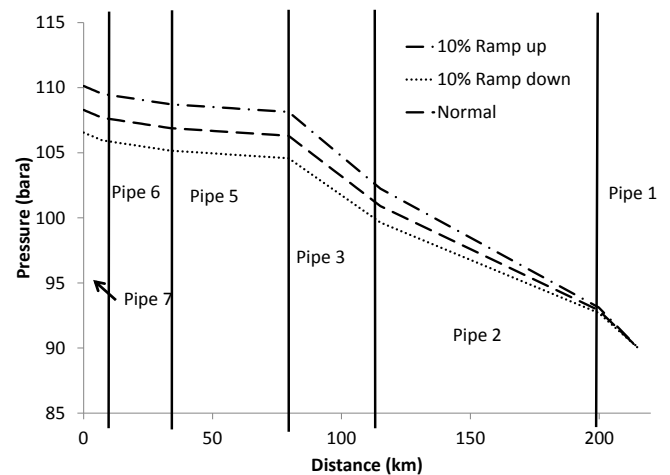

Figure 32. Variation of fluid pressure along main trunk pipeline for a 10 % ramp-up and ramp-down in the CO_2 flowrate from Drax power station for Scenario 3.

The above results demonstrate the usefulness of the model developed for analysis of the impact of variations in the network operation conditions and particularly quality of the captured CO_2 streams on the CO_2 pipeline transport.

References

Knoope, M., Guijt, W., Ramrez, A., Faaij, A., 2014. Ímproved cost models for optimizing CO_2 pipeline configuration for point-to-point pipelines and simple networks. International Journal of Greenhouse Gas Control 22, 25–46.

Brown, S., Mahgerefteh, H., Martynov, S., Sundara V. and Mac Dowell N. (2015) A Multi-source Flow Model for CCS Pipeline Transportation Networks. Accepted for publication in International Journal of Greenhouse Gas Control.

2ND INTERNATIONAL FORUM ON RECENT DEVELOPMENTS OF CCS IMPLEMENTATION

CALL FOR ABSTRACTS & REGISTRATION

Leading EC FP7 carbon capture and storage (CCS) projects CO2QUEST and IMPACTS invite you to participate in the **2nd CCS Forum**.

This event series promotes collaboration between European and International CCS research communities. In December, leading representatives from academia, industry and governing bodies will gather to share experience and knowledge, and to disseminate the latest results and technological developments in this evolving field.

The event will stimulate dialogue and will be an invaluable networking opportunity for future Horizon2020 CCS calls.

The organising committee is delighted to announce that selected papers submitted to the 2nd CCS Forum will be published in a **Special Edition of the International Journal of Greenhouse Gas Control (IJGGC)**.

The Call for Abstracts and Event Registration are now open:

Call for Abstracts

The meeting will focus on all aspects of the CCS value-chain. Abstracts are called for the following sessions:

- O Transport and Safety   O Process Optimisation and Techno-economic Considerations
- O Capture   O Thermophysical Properties
- O Combustion   O Storage

An abstract template and details of the submission process can be found on the event website.

Registration:

To register as a participant to the event please visit the event website. Registration including lunches, evening reception, and accommodation for two nights can be made at the **early-bird rate of €455**. For more information, please   contact Abby Ward (A.M.E.Ward@leeds.ac.uk) at the University of Leeds.

EVENT WEBSITE: http://goo.gl/45vfYf

DATE

Wednesday 16th and Thursday 17th December 2015

VENUE

St. George Lycabettus Boutique Hotel, Athens, Greece

REGISTRATION DEADLINE

Early bird registration is available until **31st October 2015.**

CALL FOR ABSTRACTS

We invite you to submit an abstract for either oral or poster presentation .

Deadline for submissions is the **2nd October 2015.**

FOR MORE INFORMATION, PLEASE VISIT THE EVENT WEBSITE: http://goo.gl/45vfYf

IMPACTS
The impact of the quality of CO₂ on transport and storage behaviour

CO₂QUEST
Impact of the Quality of CO₂ on Storage and Transport

Publications and Conference Participation

News regarding the up-coming CO$_2$QUEST technical workshop will be posted on the website.

http://www.co2quest.eu/

A number of papers, posters, and presentations are also available in the publications section of the project website. For regular updates on publications please visit:

http://www.co2quest.eu/publications.htm

Acknowledgement and Disclaimer

The newsletter reflects only the authors' views and the European Union is not liable for any use that may be made of the information contained therein.